Estimation of the initial amplitude of plasma bubble seed perturbation from ionograms

A. J. Carrasco[1,2] and I. S. Batista[2]

[1]Departamento de Física, Universidad de Los Andes (ULA), Mérida, Venezuela

[2]Instituto Nacional de Pesquisas Espaciais (INPE), São José dos Campos, Brazil

Corresponding author: Inez S. Batista
Instituto Nacional de Pesquisas Espaciais
Av. dos Astronautas, 1758, Jardim da Granja
12227-010 - São José dos Campos, SP, Brazil
Phone: +55-12-3208 7153
Fax:: +55-12-3208 6990
e-mail: inez@dae.inpe.br

Estimation of the initial amplitude of plasma bubble seed perturbation from ionograms

A. J. Carrasco[1,2] and I. S. Batista[2]

[1]Departamento de Física, Universidad de Los Andes (ULA), Mérida, Venezuela

[2]Instituto Nacional de Pesquisas Espaciais (INPE), São José dos Campos, Brazil

Abstract. This work gives the description of an experimental method for the calculation of the initial amplitude of plasma bubble seed perturbation in the bottomside F layer from ionograms. The observations show that after sunset the ionograms exhibit irregularities in the base of the F trace. In the context of the plasma depletion in the bottomside F-layer, the irregularities in ionograms can be seen like isodensity contour in evolution (in space and time). The initial amplitudes, calculated using the methodology, vary between 0.03 and 0.08. The ionograms analyzed were obtained from the station of Cachimbo (9.5° S, 54.8° W) during COPEX campaign in Brazil. The methodology can be useful for application in numerical simulation of plasma bubbles in which actual ionospheric parameters are used.

1. Introduction

Plasma instability phenomena occurring in the F-region of the equatorial ionosphere are grouped under the generic name equatorial spread F (ESF). Spread F, as exhibited by diffuse echoes on ionograms, was first reported in the first half of 20th century. After sunset, when the F-layer is lifted through the action of the ambient electric fields (from

F-layer dynamo), the bottomside steepens and large plasma depletions, named plasma bubbles, can be generated. A number of theoretical studies and numerical simulations have been made to understand the mechanism producing the plasma structures in the magnetic equator. The underlying plasma physics is tied to the nonlinear evolution of the generalized Rayleigh-Taylor instability (RTI) excited in the bottomside F layer. The instability can be described by a situation similar to a heavy fluid resting over a light fluid. The occurrence of a perturbation in the border between the fluids can lead to the development of instabilities and can generate irregularities in the bottomside of the F region. The evolution of these irregularities can lead to the formation of plasma bubble structures. The bubble rises through the layer in response to a Rayleigh-Taylor type instability. The bubble structures can extend hundreds of kilometers in altitude and in both hemispheres via magnetic field lines as confirmed by many experimental observations.

From October to December 2002 the Conjugate Point Equatorial Experiment (COPEX) campaign was conducted in Brazil, with the objective to investigate the equatorial spread *F*/plasma bubble irregularity (ESF) development conditions in terms of the electrodynamical state of the ionosphere along the magnetic flux tubes in which they occur. A network of instruments, including Digisondes, optical imagers, and GPS receivers, was deployed at magnetic conjugate and dip equatorial locations in a geometry that permitted field line mapping of the conjugate *E* layers to dip equatorial *F* layer bottomside. The measurements were obtained in three localities and the ionograms were taken at a 5 minutes step rate, simultaneously at the three sites. Two of these localities were the magnetic conjugate points (Boa Vista, 2.8° N, 60.7° W, and Campo Grande, 20.5° S, 54.7° W) and the third was located at the magnetic equator (Cachimbo, 9.5° S, 54.8° W) [*Abdu et al.*, 2009a; *McNamara et al.*, 2008; *Reinisch et al.*, 2004]. Using the results of the COPEX campaign, *Batista et al.* [2008] reported a velocity of rise of the order of 150 m/s for the bubbles in Cachimbo. This value corresponds to a bubble that has reached high altitude before mapping down in both hemispheres.

The observations have shown that after sunset the ionograms at the magnetic equator and low latitudes exhibit irregularities at the base of the F trace. On occasions, many discrete traces, referred in the literature as satellite traces, can be seen superposed to the main F trace, while at other times there may be no distinct structure. *Booker and Wells* [1938] interpreted these irregularities as being caused by a fast rise of F layer in the evening. The irregularities are responsible for the spread F occurrence and the rise of F layer is caused by the vertical plasma drift (pre-reversal enhancement of the zonal electric field). Several studies have suggested that the height that F layer reaches in the first hours of the night is an important parameter that controls the generation of irregularities [*Fejer et al.*, 1999]. The uplift of F layer can contribute to the destabilization of the plasma and make the instability growth rate increase with the height. Satellite traces have been frequently used as an empirical precursor of range spread F [*Abdu et al.*, 1981; *Lyon et al.*, 1961]. *Tsunoda* [2008], using ionogram and incoherent scatter radar data at an equatorial station, concluded that satellite traces in equatorial ionograms are direct signatures of large-scale wave structure (LSWS) which, in turns, is a more direct precursor of ESF than the post-sunset rise of the F layer.

The seeding mechanism of RTI in the development process of the plasma bubble has received special attention in recent investigations [see *Fritts et al.*, 2009; *Abdu et al.*, 2009b and references therein]. The coupling of the ionospheric plasma dynamics and neutral atmosphere wave dynamics has been extensively studied in the last 30 years. However, it seems that a conclusive scenario for explaining the ionosphere-atmosphere coupling dynamics, as related to spread F development, has not yet been developed. To date, the nature of the perturbation is widely believed to be gravity waves. These waves are normally generated through the process of vertical movement of air-parcels forced by convections, front activity and topography in the troposphere. These waves can propagate above 100 km, even up to 200 km in the ionosphere [*Takahashi et al.*, 2009].

In the following sections of this work, we describe an experimental method for the calculation of the initial amplitude of perturbation that can be useful for application in numerical simulation of bubbles. The ionograms analyzed correspond to the station of Cachimbo.

2. Initial amplitude

The works of *Ossakow et al.* [1979], *Ossakow* [1981], *Zalesak and Ossakow* [1980], *Zalesak* [1979] demonstrated/confirmed that a small perturbation at the base of the equatorial F region at post sunset hours leads to the formation of irregular structures. When a perturbation is present (e.g. sinusoidal) along the zonal direction (east-west) a polarization electric field is established and then the less dense (depletion) plasma moves upward. In *Ossakow et al.* [1979], the initial perturbation is defined by an analytic function in the form

$$N(x,z,0) = N_0(z)\left[1 - A\cos\left(\frac{2\pi}{\lambda}x\right)\right] \quad (1)$$

where N is the plasma density, N_0 is the background initial plasma density or equilibrium density, A is the amplitude of the initial perturbation and λ is the wavelength of the perturbation. Equation (1) represents a mesh in height (z) and horizontal (East-West) direction (x) with a maximum depression surrounding x=0. Many authors use a fixed value (5% or 0.05 in decimal) for the amplitude A in their numerical simulation of bubbles [see, for example, *Ossakow et al.*, 1979; *Huang and Kelley*, 1996a; *Sekar et al.,* 2001]. Although those authors use always a fixed value for the perturbation, it is clear that A should vary from one day to the other, because the ionospheric conditions vary on a day to day basis. Additionally, A depends strongly on the source that originates the perturbation (for example gravity waves). According to *Mendillo et al*. [1992] and *Sekar et al.* [1995] there is a significant number of observed onset conditions for the post-sunset equatorial spread F that are not evidently associated with the required (5%) seed perturbation as assumed in earlier simulation studies. Using a simulation model, *Sekar et al.* [1995] have shown that the threshold perturbation can be as low as 0.5% (or 0.005 in decimal) for the plasma bubble development. This result suggests possible values of initial amplitude smaller than 5%. The simulation works developed until now do not provide a method to calculate the parameter A.

In this work we propose an experimental method to calculate the value of parameter A from ionograms that better represent the conditions of the event to simulate. This method is described in the following session.

3. Experimental method

The initial amplitude of the perturbation can be defined as the fractional change of the electron number density *δN/N* [e.g. *Kherani*, 2002; *Sekar and Kherani*, 2002]. At the equatorial *F* region, under the RTI mechanism, this change (*δN/N*) is produced by the combination of vertical ($\vec{E}x\vec{B}/B^2$) drift and the growth of the instability. Considering a limited region in space, a positive vertical drift lifts up a portion of the layer base introducing variations in its density and height in such a way that when part of the layer base is elevated in height this is seen as a decrease in density at the same region. In the works describing numerical simulation of bubbles, this density change can be seen by the vertical rise of an isodensity contour from the base of the layer. The initial top height of the isodensity curve depends on the initial perturbation generated by the polarization field. In other words, the amplitude of the initial plasma density perturbation is an essential parameter for growth of the plasma instability under favorable conditions.

In some cases the base of the main trace (F) in ionograms can show a diffuse region. This diffuse echo (patch) has been interpreted as the signature of plasma instability. Thus the evolution of the instability can be tracked by following the movement of the irregularity at the base of the F layer trace from consecutive ionograms. Figure 1a shows a sequence of ionograms obtained in the station of Cachimbo on December 3, 2002 during the COPEX campaign. We can observe the diffuse echoes (patches) in the bottomside F trace and their displacement in frequency and height from one ionogram to the other. The accuracy with which height and frequency of the diffuse echo on main trace can be measured depends on the reading accuracy used in reducing the ionograms. In this work the convention adopted for reading the upper frequency limit of the diffuse echo is that it should be contiguous to the $h'(f)$ trace (see the vertical arrows in Fig.

1a). The upper limit of the echo corresponds to the top height of the isodensity curve in Figure 1b, according to the following reasoning: as the irregularity (bubble) evolves it grows in height inside the F layer (the top of the isodensity curve reaches distinct heights at different times). In the ionograms this movement is seen as a bi-dimensional (height and frequency) evolution of the top of the irregularity (bubble) over the ionogram main trace, which means equivalence between the position in space and time of the top of the irregularity and the isodensity curve top. In this way, after a time lag t, the new vertical position of the top of an isodensity curve will be detected in the ionogram as a frequency variation as the top of the irregularity evolves above the main trace. Under this assumption, once the frequency evolution is known, we can obtain the new height of the irregularity over the trace. The Digisonde precision for measuring virtual height is ±5 km but the Sao-Explorer program [*Galkin et al.,* 2008] can interpolate values with 0.1 km of precision. However, we must be careful not to confuse precision and observational error in the virtual height.

For the sequence of ionograms in Fig. 1 the values obtained for height and frequency at the upper end of the patch, marked by horizontal and vertical arrows, respectively, in the ionograms, are (t_0=22:40 UT, no diffuse echo, only satellite trace seem as precursor of the instability), (t_1=22:45 UT, h_1=380.6 km, f_1=2.0 MHz), (t_2=22:50 UT, h_2=399.2 km, f_2=2.2 MHz), (t_3=22:55 UT, h_3=413.6 km, f_3=2.4 MHz). The frequencies f_i are obtained at the upper limit of the diffuse echo in each ionogram and the heights h_i correspond to the virtual height at the frequency f_i $(h_i = h'(f_i))$. In the context of the plasma depletion in the bottomside F-layer, the irregularities or structures can be seen as isodensity contour in evolution, where the plasma decrease rate is associated with the rate of change in height of the isodensity contour (Figures 1a and 1b). In Figure 1b the sequence of isodensity curves represents the height evolution of the irregularity seen in part (a) of the figure. The heights marked with arrows correspond to the height at the limit of frequency of a diffuse echo on the main profile of density (ionogram). In Figure 1c the sequence of profiles represents a schematic of the time evolution of the vertical electron density profiles as the irregularity develops. To determine the initial amplitude A we assume a linear development of the irregularity during its initial phase in such a way that the fractional change of the electron number density, $\delta N/N$, can be calculated from the rate of change (or fractional variation) in virtual height of two consecutive positions of upper limit of the diffuse echo, that is $\delta N / N \approx \Delta h / h$. Thus the initial amplitude can be calculated from the expression $A \approx h_2 / h_1 - 1$. As an example of the method, using the data from Figure 1a, h_1=380.6 km, h_2=399.2 km we obtain $A = 0.048$ and the vertical velocity of the irregularity $\left(h_3 - h_1\right)/ 2\Delta t = 55 m / s$. This velocity is the result of the action of two electric fields: the ambient electric field (E_0) and the electric field of the perturbation (E_1). The perturbation electric field (E_1) is not easy to measure directly at the moment that the irregularity arises. In a first approach, E_1 can be obtained from the numerical solution of the differential equation for the perturbation electrical potential (Φ_1). On the other hand, in the differential equation the source term depends on the ambient electric field and on the collision frequency in the form $1/\nu_i$. These two parameters can influence the numerical solution of the electrical potential. Additionally, the perturbation in the density evolves according to the RTI growth rate, γ [for more details see, for example, *Huang and Kelley*, 1996a].

From the technical point of view our observations were limited to the presence of irregularities visible in the ionograms at frequencies larger than 1.5 MHz. During the night the F trace is visible from 1.5 MHz onwards (on average). Under these conditions, if irregularities are present at frequencies less than 1.5 MHz they can not be detected with the technique of vertical sounding. We have applied the described method to 10 days of data obtained at the equatorial station Cachimbo during the COPEX campaign.

4. Results and discussion

The results of the experimental method used to calculate the amplitude *A* of the initial perturbation are shown in Table 1 for different events observed in Cachimbo, together with other relevant parameters such as the spread-F onset time (TimeI) and the time of occurrence of the maximum in the vertical drift pre-reversal enhancement (TimeP), the Dst index and the solar flux at 10.7 cm (F10.7). The values obtained for the initial amplitude (*A*) vary between approximately 0.03 and 0.08. The irregularity onset time (TimeI) varies between 22:10 and 23:15 UT. Comparing TimeI and TimeP, it is possible to conclude that the irregularities initiate only after the vertical drift, V_0, reaches its maximum value (Vp), as already reported by *Nelson et al.* [1986]. In Figure 2 we plot the amplitude versus the perturbation electric field. The perturbation electric field was calculated based on the assumption that the total electric (E) responsible for the bubble rise is equal to the sum of the ambient electric field (E_0) and the perturbation electric field (E_1). Around sunset the ambient electric field can be calculated from the vertical drift according to the expression $\Delta h'F / \Delta t \approx E_0 / B$ [*Bittencourt and Abdu*, 1981; *Batista et al.*, 1986], where $h'F$ is the minimum virtual height of the F layer, t is time and B is the geomagnetic field. Similarly the total electric field (E) responsible for the bubble rise can be obtained from the expression $\Delta h_C / \Delta t \approx E / B$, where

$\Delta h_C = h'(f_j) - h'(f_i)$. In Figure 2 even with so few points we can observe a definite dependency of the behavior of the amplitude with the perturbation field (E_1). The two curves plotted in the graphic represent linear and power fitting to the data. This result represents an effort to obtain the initial amplitude and the perturbation electric field at the beginning of the irregularities. According to our results, it seems that there is a threshold (approximately equal to 0.03) in the relative amplitude above which irregularities/bubbles can be generated in the equatorial ionospheric region under study. This threshold is lower than that used by some author in theoretical simulation of plasma bubbles, but is not as low as that found in the work of *Sekar et al*. [1995], that found a threshold of 0.005. As we have used an experimental methodology to determine the threshold, it is possible that time and/or height resolution of our data introduce limitations in determining thresholds lower than 0.03. Another possibility for the higher threshold found in the present work as compared to *Sekar et al*. [1995] is the dataset used in the present study, that does not show the very high upward drift velocity needed for the plasma bubble development with the low threshold found by *Sekar et al*. [1995]. The verification/validation of those hypothesis can be clarified with the aid of a numerical simulation code of bubbles in which all the atmospheric/ionospheric parameters are known (vertical profile of plasma, neutral temperature, electric field, collision frequency, etc), and the amplitude varies from one simulation to the other. We do not try to infer the nature of the seed perturbation in the present study but only to show the effect of the initial amplitude and its correlation with other atmospheric parameters. The combination of the parameters, A, E_1, ν_i (collision frequency) can play an important role in the determination of the onset time of occurrence of the irregularities.

Figure 3 shows the temporal variation of the vertical drift for three events. In order to facilitate the analysis of this figure, we will compare first events on 16 and 29 of November. In this figure we can observe that the peak of the vertical velocity, Vp is higher in the event of day 16 (56 m/s) than in the November 29 event (46 m/s) but the irregularity starts earlier in the event of day 29 (see Table 1). For this discussion we will need the expression for the linear growth rate (horizontal mode of propagation and without neutral wind) which is given by [*Huang and Kelley*, 1996a]

$$\gamma = \frac{1}{N_0}\frac{\partial N_0}{\partial z}\left(\frac{g}{\nu_i} + \frac{E_0}{B}\right) - \beta \qquad (2)$$

where g is the acceleration due to gravity, ν_i is the collision frequency and β is the recombination coefficient. Based on this equation, γ increases when ν_i decreases. The minimum F layer virtual heights at the time of the perturbation onset in the ionogram were, respectively, 423 and 342 km on the 16 and 29 November, but between 2100 and 2200 UT the heights were very similar on both days. According to various simulation works the instability begins to grow 20 to 30 minutes after the perturbation in the bottomside starts. This time lag that the phenomenon takes to evolve and to be observed in the ionograms is an important point to be considered. In Figure 3 we can observe that the drift velocity between 21:00 and 22:00 UT is very similar in the events on 16 and 29 November. Under these circumstances the bottomside F layer vertical rise was similar in the two days. This can suggest that, for these particular events, the ambient electric field, E_0, does not fully control the evolution of the instability. Nonetheless its contribution is important in the development of the structures, when the perturbation occurs in the bottomside. In Table 1 we can see that the solar flux was larger in the event of November 16 as compared to November 29. The increase of neutral temperature with the solar flux can increase the collisions between neutral particles with ions [see for example, *Schunk and Nagy*, 2009] contributing to the decrease of g/ν_i on 16 Nov as compared with 29 Nov. This could decrease the instability growth rate and hence cause a delay in the time of occurrence of the irregularities. Under these conditions the 29 Nov event should evolve faster compared to the 16 Nov event, as indeed observed. On the other hand, at the time of the irregularity onset, the layer is higher on the 16th than on the 29th, which could compensate the increase in collision frequency due to temperature increase on 16th. Additionally, it is important to emphasize that γ represents a measurement of the evolution of the instability when the initial density perturbation occurs. The difference of initial amplitude between the events can also play an important role in the development of the instability. As noted from Table 1, the amplitude A is twice larger on 29th as compared to the 16th, suggesting that initial density perturbation is larger on 29th. *Abdu et al.* [2009] and *Kherani et al.* [2009] have shown that for similar electric field strength as here (56 and 46 m/s on 16th and 29th, respectively), the bubble growth is larger when the initial amplitude is large. On this basis it is expected that on 29th bubble will grow faster. In this context, the results presented here are the first to directly estimate the parameter A based on ionograms and relate it with the bubble growth on two nights.

Figure 4 shows a plot of the variation of delay (the difference between TimeI and TimeP) with the perturbation amplitude. In the figure we can see that the delay decreases with the increase of the amplitude (a linear and exponential fit to the data points are also shown in the figure). This interesting result suggests a straight relationship between the hour of occurrence of the irregularity and the amplitude of the initial perturbation in density, A.

The event that showed the largest delay (~1 hour) occurred on October 27. This large delay between the peak of the vertical velocity and the beginning of the irregularity can be attributed to a low value of E_0 or V_0 (surrounding the maximum) probably caused by a magnetic disturbance (Dst= -61). The initial amplitude for the 27 Oct event was very similar to the event on 16 Nov (~0.03) but the delay was ~30 min larger in the first event as compared to the second. In order to support the theory about the effect of the electric field, E_0 and collision frequency, we analyzed the event of 14 Oct (not included in Table 1). For the 14 Oct event (Dst= -60, F10.7= 180) the maximum pre-reversal vertical drift was Vp = 23 m/s at 22:10 UT and did not present/display irregularities. Comparing the events of 14 and 27 Oct it is evident that the low value of the vertical drift (23 m/s) affected the development of the instability. According to *Huang and Kelley* [1996b], the equatorial electric fields associated with magnetic storms cannot produce plasma bubbles when the F layer is low. This is because the growth rate of the Rayleigh-Taylor instability is low for low F layer height. In comparison with the previous explanation, *Woodman* [1994] argued that the plasma bubbles could be seeded by the prereversal enhancement of the east-west electric field.

5. Conclusions

The main purpose of this work was the development of an experimental method for the calculation of the initial amplitude of perturbation. Our results showed a variation between 0.03 and 0.08 for the fractional change in the number density in the bottomside of the F-region. A threshold of 0.03 was found for the initial amplitude of perturbation, necessary for the development of irregularities in the equatorial ionospheric region under study. It is possible that lower threshold values, compatible with the results by *Sekar et al*. [1995] could be attained if the methodology was applied to distinct data sets with different time and height resolution. An important result was the linear relationship between the hour of occurrence (or delay) of the irregularity and the initial amplitude showing that the delay tends to decrease with the increase of the initial amplitude. The results presented here are the first to directly estimate the parameter *A* based on ionograms and relate it with the bubble growth on two nights. Motivated by the obtained results, the experimental method will be applied to other ionospheric stations over the magnetic equator and will be used in numerical simulation with the intention to simulate the time of occurrence of the bubbles experimentally detected.

Acknowledgements. The authors wish to acknowledge the support from FAPESP through the process 2010/05698-8 through which the visit of Dr. Carrasco to the Aeronomy Division, DAE/INPE was made possible. The authors thank the referees for their useful comments.

References

Abdu, M. A., I. S. Batista, and J. A. Bittencout (1981), Some characteristics of equatorial spread F at the magnetic equatorial station Fortaleza, *J. Geophys. Res*., 86, A8, 6836-6842.

Abdu, M. A., I. S. Batista, B. W. Reinisch, J. R. de Souza, J. H. A. Sobral, T. R. Pedersen, A. F. Medeiros, N. J. Schuch, E. R. de Paula, and K. M. Groves (2009a), Conjugate Point Equatorial Experiment (COPEX) campaign in Brazil: Electrodynamics highlights on spread F development conditions and day-to-day variability, *J. Geophys. Res*., 114, A04308, doi:10.1029/2008JA013749.

Abdu, M. A., E. A. Kherani, I. S. Batista, E. R. Paula, D. C. Fritts, and J. H. A. Sobral

(2009b), Gravity wave initiation of equatorial spread F /Plasma bubble irregularities based on observational data from the SpreadFEx campaign, *Ann. Geophys.*, *27*, 2607-2622.

Batista, I. S., M. A. Abdu, J. A. Bittencourt (1986), Equatorial F region vertical plasma drifts: Seasonal and longitudinal asymmetries in the American sector, *J. Geophys. Res.*, *91*, 12,055-12,064.

Batista, I. S., M. A. Abdu, A. J. Carrasco, B. W. Reinisch, E. R. Paula, N. J. Schuch, and F. Bertoni (2008), Equatorial spread F and sporadic E-layer connections during the Brazilian Conjugate Point equatorial Experiment (COPEX), *J. Atmos. Sol. Terr. Phys.*, *70*, 1133-1143, doi:10.1016/j.jastp.2008.01.007.

Bittencourt, J. A., and M. A. Abdu (1981), A Theoretical comparison between apparent and real vertical ionization drift velocities in the equatorial F region, *J. Geophys. Res.*, *86,* A4, 2451-2454.

Booker, H. G., and H. W. Wells (1938), Scattering of radio waves in the F-region of the ionosphere, *Terr. Magn. Atmos. Electr.*, *43*, 249-256.

Fejer, B. G., L. Scherliess, and E. R. Paula (1999), Effects of the vertical plasma drift velocity on the generation and evolution of equatorial spread F, *J. Geophys. Res.*, *104,* A9, 19859-19869.

Fritts, D. C., M. A. Abdu, I. S. Batista, P. P. Batista, R. Buriti, B. R. Clemesha, T. Dautermann, E. R. de Paula, J. Fechine, B. G. Fejer, D. Gobbi, J. Haase, F. Kamalabadi, E. A. Kherani, B. Laughman, P. P. Lima, H.-L. Liu, A. Medeiros, P.-D. Pautet, D. M. Riggin, F. S. Rodrigues, F. São Sabbas, J. H. A. Sobral, P. Stamus, H. Takahashi, M. J. Taylor, S. L. Vadas, F. Vargas, and C. M. Wrasse (2009), Overview and summary of the Spread F Experiment (SpreadFEx), *Ann. Geophys., 27*, 2141–2155.

Galkin, I. A., G. M. Khmyrov, B. W. Reinisch, and J. McElroy (2008), The SAOXML 5: New format for ionogram-derived data, in *Radio Sounding and Plasma Physics, AIP Conf. Proc. 974*, 160-166.

Huang, C. S., and M. C. Kelley (1996a), Nonlinear evolution of equatorial spread F: Gravity wave seeding of Rayleigh-Taylor instability, *J. Geophys. Res.*, *101,* A1, 293-302.

Huang, C. S., and M. C. Kelley (1996b), Nonlinear evolution of equatorial spread F. Plasma bubbles generated by structured electric fields, *J. Geophys. Res.*, *101,* A1, 303-313.

Kherani, E. A., Investigations of F region plasma instabilities under different background conditions, Ph.D. thesis, 92 pp., Mohanlal Sukhadia Univ., Udaipur, India, 2002.

Kherani, E. A., M. A. Abdu, E. R. de Paula, D. C. Fritts, J. H. A. Sobral, and F. C. de Meneses Jr. (2009), *Ann. Geophys.*, *27*, 1657-1668.

Lyon, A. J., N. J. Skinner, and R. W. Wright (1961), Equatorial spread F at Ibadan, Nigeria, *J. Atmos. Terr. Phys.*, 21, 100.

Mendillo, M., J. Baumgardner, X, Pi, P.J., Sultan, and R. T. Tsunoda (1992), Onset conditions for equatorial spread F, *J. Geophys. Res.*, *97*, doi:10.1029/92JA00647, 13865-138761.

McNamara, L. F., J. M. Retterer, M.A. Abdu, I. S. Batista, B. W. Reinisch (2008), F2 Peak parameters, drifts and spread F derived from digisonde ionograms for the COPEX campaign in Brazil, *J. Atmos. Solar-Terr. Phys. 70.* 1144–1158.

Nelson, O. R., M. A. Abdu, and I. S. Batista (1986), Equatorial F-region irregularity latitudinal extension and dynamo electric field, *J. Atmos. Terr. Phys.*, *48*, 2, 181.

Ossakow, S. L. (1981), Spread F theories-a review, *J. Atmos. Terr. Phys.*, *43*, 5/6, 437-452.

Ossakow, S. L., S. T. Zalesak, and B. E. McDonald (1979), Nonlinear Equatorial Spread F: Dependence on Altitude of the F Peak and Bottomside Background Electron Density Gradient Scale Length, *J. Geophys. Res.*, *84*, A1, 17-29.

Reinisch, B. W., M. Abdu, I. Batista, G. S. Sales, G. Khmyrov, T. A. Bullett, J. Chau, and V. Rios (2004), Multistation digisonde observations of equatorial spread F in South America, *Ann. Geophys. 22*, 3145–3153.

Schunk, R., and A. Nagy (2009), *Ionosphere Physics, Plasma Physics, and Chemistry*, Cambridge.

Sekar, R., and E. A. Kherani (2002), Effects of molecular ions on the collisional Rayleigh-Taylor instability: Nonlinear evolution, *J. Geophys. Res.*, *107*, A7, 1139-1147, doi: 10.1029/2001JA000167.

Sekar, R., E. A. Kherani, P. B. Rao, and A. K. Patra (2001), Interaction of two long-wavelength modes in the nonlinear numerical simulation model of equatorial spread F, *J. Geophys. Res.*, *106*, A11, 24,765-24,775.

Sekar, R., R. Suhasini, and R. Raghavarao (1995), Evolution of plasma bubbles in the equatorial F region with different seeding conditions, *Geophys. Res. Lett.*, *22*, 885-888.

Takahashi, H., M. J. Taylor, P.-D. Pautet, A. F. Medeiros, D. Gobbi, C. M. Wrasse, J. Fechine, M. A. Abdu, I. S. Batista, E. Paula, J. H. A. Sobral, D. Arruda, S. L. Vadas, F. S. Sabbas, and D. C. Fritts (2009), Simultaneous observation of ionospheric plasma bubbles and mesospheric gravity waves during the SpreadFEx Campaign, *Ann. Geophys.*, *27*, 1477-1487.

Tsunoda, R. T. (2008), Satellite traces: An ionogram signature for large-scale wave structure and a precursor for equatorial spread F, *Geophys. Res. Lett*., 35, L20110, doi:10.1029/ 2008GL035706.

Woodman, R. F. (1994), Equatorial ionospheric irregularities as observed by the Jicamarca radar, in Low-Latitude Ionospheric Physics, F. S. Kuo, Pergamon, New York.

Zalesak, S. T. (1979), Fully Multidimensional Flux-Corrected Transport Algorithms for Fluids, *J. Comput. Phys*., *31*, 335-362.

Zalesak, S. T., and S. L. Ossakow (1980), Nonlinear Equatorial Spread F: Spatially Large Bubbles Resulting From Large Horizontal Scale Initial Perturbations, *J. Geophys. Res*., *85*, A5, 2131-2142.

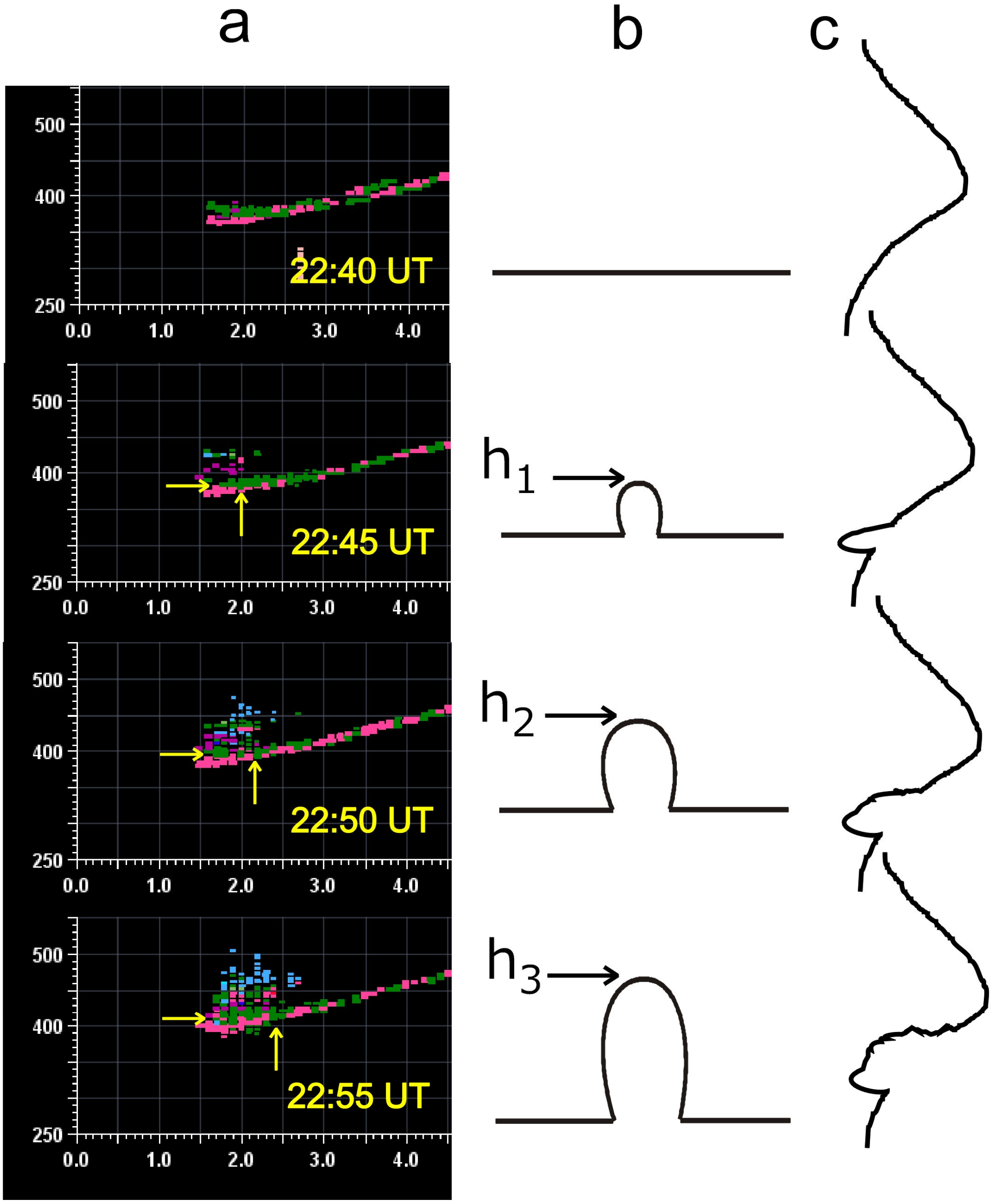

Fig. 1 Illustrative description of the experimental method applied to the ionograms for December 3, 2002 from 22:40 to 22: 55 UT. In part (a) of the figure we can see, from the ionograms, the growth of the irregularity at the base of F layer. Part (b) illustrates the isodensity contour corresponding to each ionogram. Part (c) shows a schematic illustration of the electron density vertical profile.

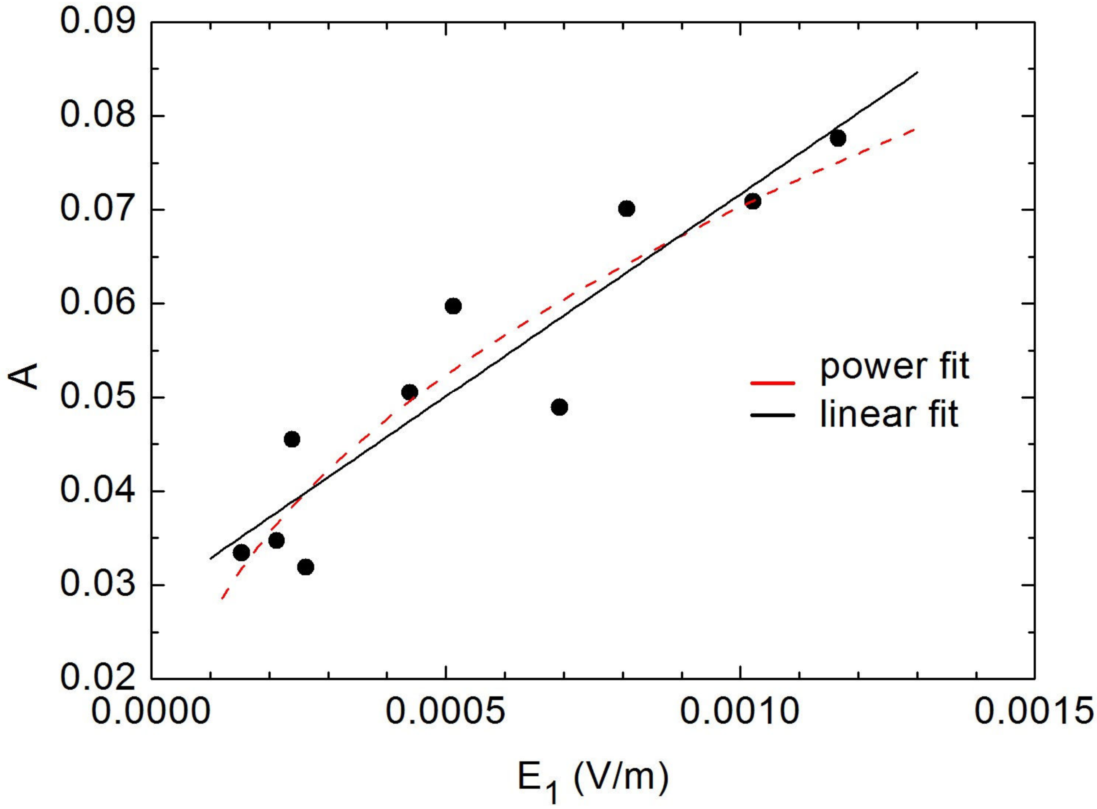

Fig. 2 Variation of the amplitude with the perturbation electric field. Two functions were fit to the data.

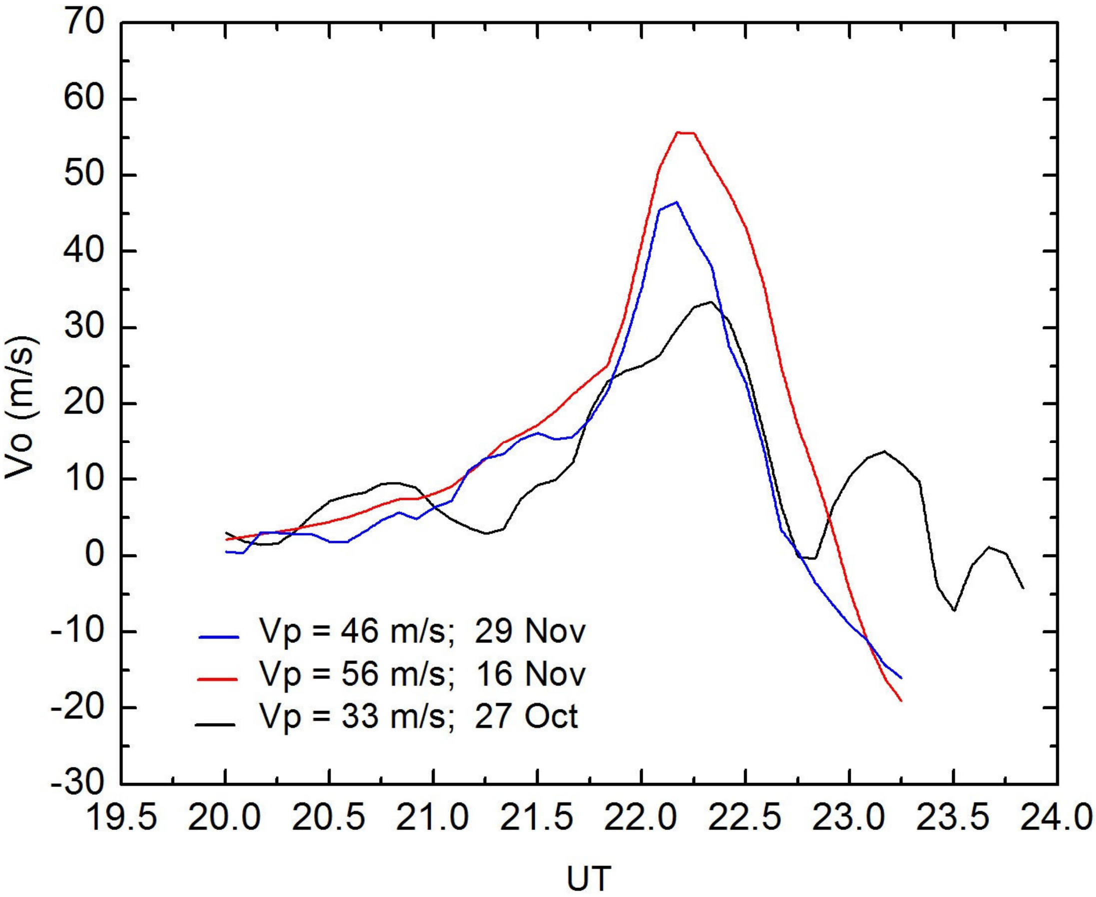

Fig. 3 Variation of the vertical plasma drift as a function of the hour (UT) for three days over Cachimbo from data collected during the COPEX campaign.

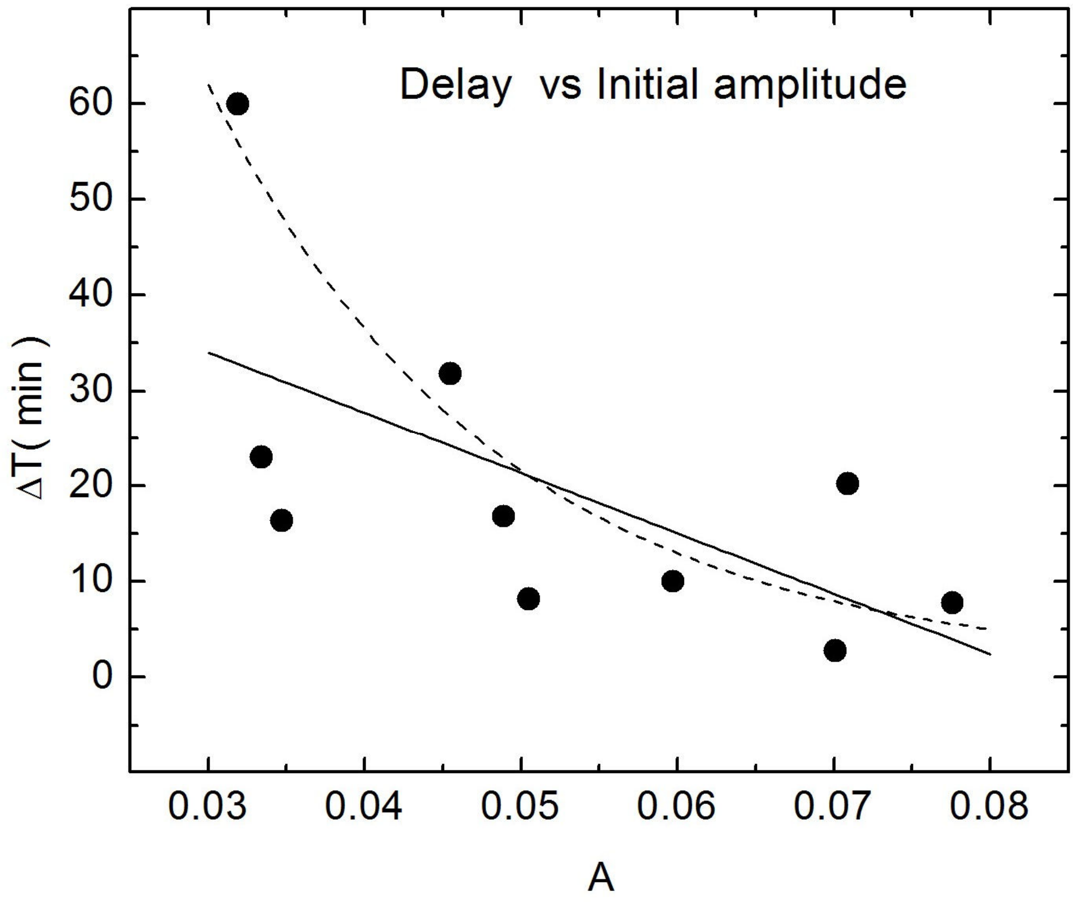

Fig. 4 Variation of the delay with the initial amplitude of perturbation. Two functions were fit to the points. The delay decreases as the amplitude increases.

Table 1
List of the events used in the study

Event	TimeI (UT)	TimeP (UT)	Dst	F10.7	A
6 Oct 2002	22:30	21:58	-60	161.7	0.0455
8 Oct 2002	22:25	22:05	-53	165.4	0.0709
11 Oct 2002	22:05	21:49	-35	179.4	0.0347
22 Oct 2002	22:10	22:02	-19	173.3	0.0505
27 Oct 2002	23:15	22:15	-61	157.1	0.0319
6 Nov 2002	22:25	22:15	-51	184.5	0.0597
13 Nov 2002	22:15	22:07	-31	167.1	0.0776
16 Nov 2002	22:30	22:07	-28	196.1	0.0334
29 Nov 2002	22:10	22:07	-23	143.0	0.0701
3 Dec 2002	22:45	22:28	-21	148.3	0.0489